研 究 者：Kiyomi Yoshida（所属：Department of Anesthesiology, Nihon University School of Dentistry at Matsudo）

研究題目：Circadian clock dysfunction alters bone homeostasis

目　的：

Aging is associated with dysfunctions in multiple organs, especially liver, and bone. Dysregulation of the molecular clockwork of aging could be ascribed to the mechanism of transcription factor DEC1, a marker of aging. However, little is known about the specific microRNA（miRNA）changes that control the pathophysiological processes of bone aging. We aimed to explore miRNA expression profiles and gain insight into molecular mechanisms of aging of femur.

対象および方法：

Bone mineral density（BMD）and BMD color imaging were performed to quantify and visualize the bone density. The femur was subjected to microcomputed tomography（mCT）scanning performed with an R_mCT2 device（Rigaku Corp., Tokyo, Japan）using a 90-kV anode electrical current at a 30-μm resolution. The isotropic voxel resolution was 30 μm × 30 μm × 30 μm. R_ mCT Image Analysis software（Rigaku Corp., Tokyo, Japan）was used to generate three-dimensional models using the scanned data. A TRI/3DBON image analyzer（Ratoc System Engineering Co., Ltd., Tokyo, Japan）was used to calculate the BMD of the bone and generate color images depicting BMD intensity, with blue and light blue, green and yellow, and orange and red representing low, medium, and high BMD values, respectively. Three-months old and 24-months old of C57BL/6（WT）mice and Dec1KO mice were used and total RNAs were isolated from their femur tissues. miRNA expression was analyzed by mouse miRNA array analysis and subsequent validated with quantitative RT-PCR. The targets of the significantly different miRNAs were predicted with miRNA prediction databases, and pathway analysis of the predicted target genes was performed using bioinformatics resources（GeneSpring, Ingenuity Pathways Analysis, and TargetScan）.

結　果：

Compared with young bones, aged bones displayed significant decreases in bone mass indicated by the reduced micro-CT parameters of BV/TV, Tb.N, and CBT（Fig. 1A-G）. Histological analysis showed a decreased number of osteocytes and an increased number of empty lacunae in aged relative to young cortical bone（Fig.1L）. Compared with young bone, the inner surface of aged cortical bone was less smooth with more visible resorption pits, below which empty lacunae were easily observed（Fig.1H-K）. To further investigate the

condition of the extracellular matrix, Toluidine Blue, Masson, and Azan staining were performed. The results showed abundant dendrites connecting into a network around young osteocytes in young bone（Fig.1M）, while continuous dendrites were rare in aged cortical bone（Fig.1N）. Masson staining revealed predominantly blue staining in young cortical bone（Fig. 1O）; in aged bone, however, bone matrix was mainly stained in red（Fig. 1P）, indicating a change in collagen composition in bone matrix during ageing. Azan staining demonstrated poor densification and loose tissue structure of collagen fibers in aged bone matrix（Fig. 1Q, R）. The alveolar bone resorption was significantly increased in aged mice and the abrasion of molar teeth was occurred in aged mice compared to young mice（Fig 2）. Profiles and Frequencies of CD3+ T cell subset and B220+ B cell subset in aged Dec1KO mice and H-E staining and micro CT analysis of Femur have been analyzed（Fig. 3, 4）. Eleven miRNAs were significantly different in the femur of aged Dec1KO mice compared to the aged WT mice, including 6 miRNAs that were up-regulated and 5 miRNAs that were down-regulated（Fig. 5）. Functional analysis indicated that many pathways potentially regulated by these miRNAs were involved in metabolism signaling, AMPK signaling, mitochondrial dysfunction, epithelial-mesenchymal transition pathway, and sirtuin signaling pathway.

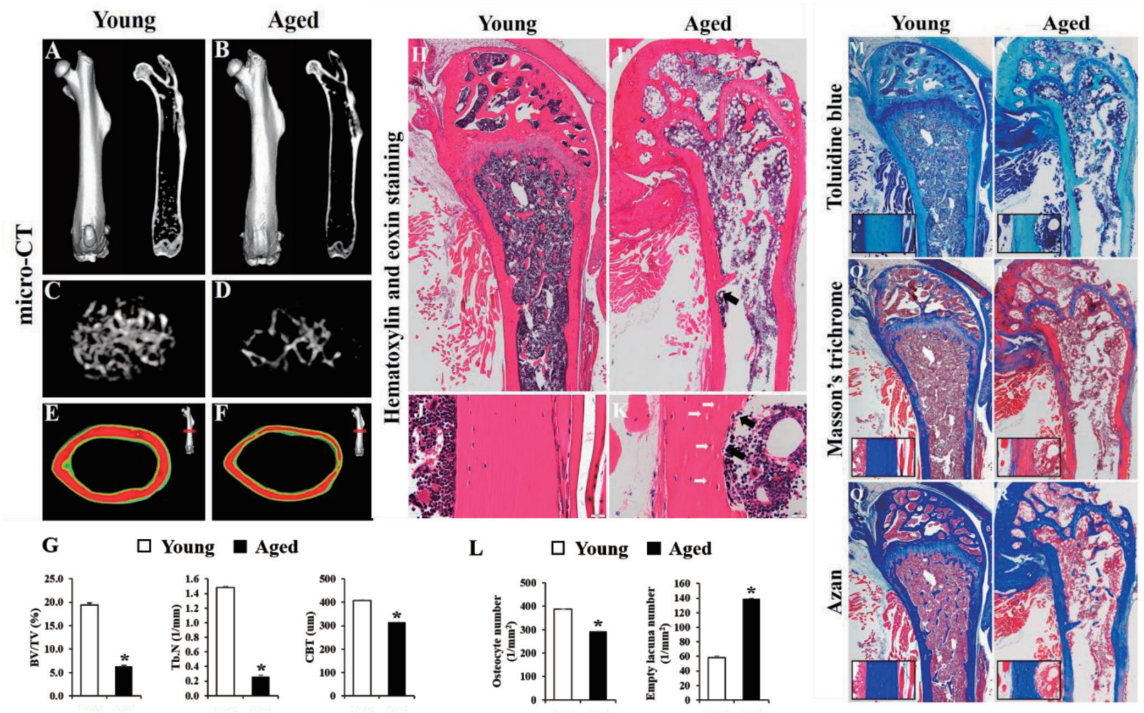

Figure 1　Aging-related changes of bone and bone matrix in WT mice

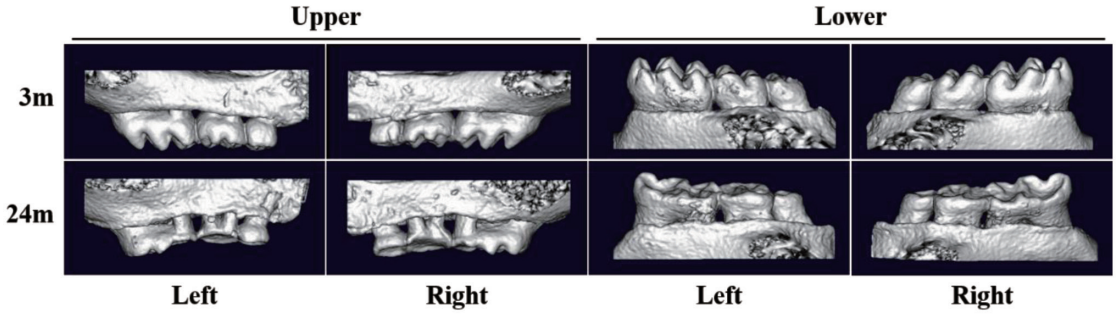

Figure 2　The resorption of the alveolar crest in the upper and lower jaws of young and aged WT mice

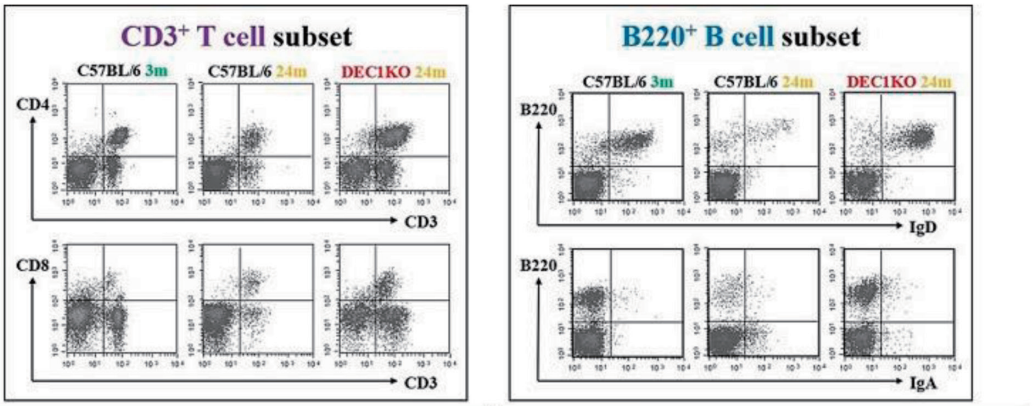

CD3⁺ T cell in aged DEC1 KO mice

Tissue	Mouse	% of Lymphocytes: CD3	% of CD3⁺ Lymphocytes: CD3⁺/CD4⁺	CD3⁺/CD8⁺
	C57BL/6 3m	34.08 □2.35	56.08 □0.38	03.22 □0.23
	C57BL/6 24m	11.03 □2.2	38.55 □7.15	27.18 □3.6
	DEC1KO 24m	51.81 □6.59	61.41□0.15	15.95 □1.73

B220⁺ B cell in aged DEC1 KO mice

Tissue	Mouse	% of Lymphocytes: B220	B220⁺/IgD⁺	B220⁺/IgA⁺
	C57BL/6 3m	19.34 □0.06	86.81 □0.7	03.81 □1.1
	C57BL/6 24m	04.99 □0.19	55.52 □6.45	19.34 □2.0
	DEC1KO 24m	31.53 □0.2	89.92 □1.62	10.1 □2.44

Figure 3　Profiles and frequencies of CD3＋ T cell subset and B220＋ B cell subset in aged Dec1 KO mice

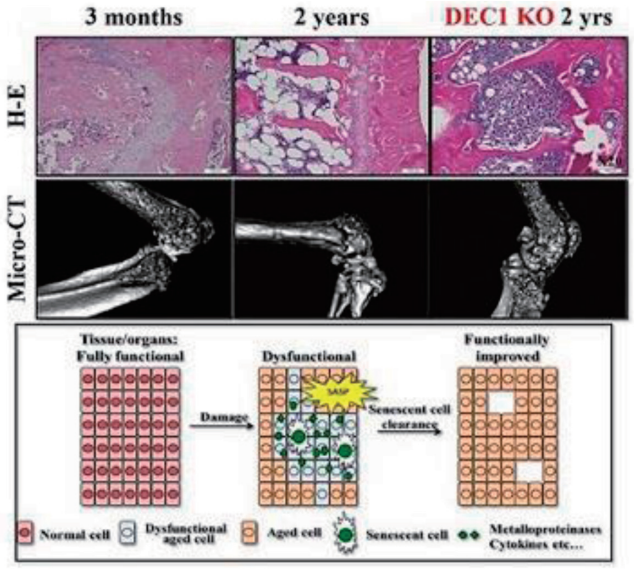

Figure 4　H-E staining and micro CT analysis in aged Dec1KO mice

miRNA	Fold Change	Target Genes
Down-regulated		
miR-a	-629.65	ATF6,CCND1,CCNE1,CCNE2,CCNF,CDC14A,CDC25A,CDKN1A,CHEK1,FGF2,FGFR1,WEE1
miR-b	-20.77	FGF16,HMOX1,KIT,NCL,PTEN,SCN3A,VSNL1
miR-c	-9.63	ARHGAP32,CAPN8,MECP2,MMP9,PGC,RB1,SOX4,TJP1
miR-d	-3.97	BCL2,BCL2L11,BMPR2,BNIP2,CCND1,CCNE1,CDKN1A,CREB1,CXCL8,E2F1,E2F2,E2F3,EGR2,MMP3,PPARG,PTEN,RHOA,RUNX1,RUNX2,STAT3,TGFBR2,TLR7,TNF,TP63,TUSC2,VEGFA,VIM
miR-e	-3.81	ARL5A,CPEB4,HECTD2,LRIG3
miR-f	-3.48	AKT1,CCNE1,CDC42,CDK6,CORO2B,HMGA2,RHOA
miR-g	-2.55	ALCAM,ARHGDIA
miR-h	-2.38	AQP4,HSPB6,IGF1,TAGLN,VIM
miR-i	-2.30	AICDA,BACH1,CEBPB,CSF1R,EGR2,MYB,PDGFB,VEGFA
miR-j	-2.24	BCL2L12
miR-k	-2.16	AR
miR-l	-2.10	HDAC5

miRNA	Fold Change	Target Genes
Up-regulated		
miR-A	3462.66	RHOA
miR-B	2156.18	BCL2,BDNF,CDK14,CDK9,CLCN3,EGFR,IGF1,NOTCH2,NOTCH3,TIMP3
miR-C	700.82	AQP4,CDK6
miR-D	604.92	SUFU,TUSC2
miR-E	532.22	CCND1,E2F6,ESR1,ETS1,MCL1,PLAU,PTK2
miR-F	442.54	DHFR,DTL,IGF1,IGF1R,TYMS,ZEB1,ZEB2
miR-G	399.85	KIT,SLC45A3
miR-H	355.70	ALOX5,CD14,ELOVL7,ENPP6,PLCG2,TNFRSF1B
miR-I	347.27	GLI1,RUNX1,SMO,SRF
miR-J	329.51	AR
miR-K	264.01	AURKB,BMP1,CDC25B,CDH11,MMP3,MMP9,PPARG,SOX4,SPARC
miR-L	235.70	ABCA1
miR-M	162.91	CCND1,CCND3,EGR2,FGF16,FGFR3,IGF1R,MMP13,MTOR,PLK1,RPTOR,SMARCA5
miR-N	143.77	BCL2,BMI1,CD69,CDKN1B,GATA6,HOXA11,KRAS,MMP14,NOTCH4,TIMP3
miR-O	126.53	FOXO1,TWIST1,VIM
miR-P	122.08	BCL2L1,CD47,ETS1,SMO
miR-Q	89.86	AXIN2,BCL2,CCND1,CD47,CDC25A,CDK6,CDKN1A,CREB1,E2F1,E2F2,E2F3,E2F5,FOXP1,HDAC1,ICAM1,JAG1,KLF4,MAP2K1,MET,MYB,MYC,MYCN,NOTCH1,NOTCH2,PPARG,SIRT1,TP53,VEGFA,WNT1
miR-R	88.82	APAF1,BCL2L11,BNIP3L,CDKN1B,CDKN1C,DDIT4,FOXO3,ICAM1,KIT,MMP1,PIK3R1,PPP2R2A,PTEN,PTPRM,SOD2,TBK1,TIMP3

Figure 5：microRNA array and target genes in bone aging

結　論：

With the comprehensive analysis of mRNAs and miRNAs, a great number of pairs have been identified, suggesting abnormally expressed miRNAs have functions in the salivary glands aging, and the function may be achieved through the post-transcriptional regulation of certain genes on the related pathways.

（A-F）Representative micro CT images：overall views（A, B），trabecular views（C, D），and cross section views（E, F）of young（3-months old）and aged（24-months old）mouse femurs.（G）Micro CT measurements for bone volume to total volume ratio（BV/TV），trabecular number（Tb.N），and cortical bone thickness（CBT）in mouse femurs.（H-K）Representative images of H-E staining of mouse femurs：low magnification（H, I）and high magnification of cortical bone area（J, K），young and aged. White arrows（K）indicate the empty lacunae, and black arrows indicate the resorption pits（I, K）.（L）The osteocyte and empty lacuna count per unit area in the young and aged cortical bone.（M, N）Representative images of Toluidine Blue staining of cortical bone, young and aged.（O-R）Distribution of collagen in the bone indicated by Masson's trichrome（O, P）and Azan staining（Q, R）. young and aged. Data in all bar plots are shown as means ± SD, $^{*}P < 0.05$.

成果発表：（予定を含めて口頭発表、学術雑誌など）

Presentation：

1. MicroRNA expression profiling and functional analysis of dysregulated microRNAs in bone aging. Ujjal K. Bhawal, Fengzhu Zhang, Kiyomi Yoshida, Makoto Makishima, Koh Shibutani, Koichi Hiratsuka. 97th IADR Meeting, Vancouver, Canada. June 19-22, 2019；poster presentation.

Publication：

1. Effects of 830 nm low-power laser irradiation on body weight gain and inflammatory cytokines in experimental diabetes in different animal models. Ujjal K. Bhawal, Kiyomi Yoshida, Takashi Kurita, Masatoshi Suzuki, Yuichiro Okada, Nitesh Tewari, Shunichi Oka, Noboru Kuboyama, Koichiro Hiratsuka. Laser Therapy 2019；28（4）：257-265.